
Efficient Transient Noise Analysis in Circuit Simulation

Georg Denk¹, Werner Römisch², Thorsten Sickenberger², and Renate Winkler²

¹ Qimonda AG, Products, München, Germany, georg.denk@qimonda.com

² Institute of Mathematics, Humboldt-Universität zu Berlin, Germany,
{romisch/sickenberger/winkler}@math.hu-berlin.de

Transient noise analysis means time domain simulation of noisy electronic circuits. We consider mathematical models where the noise is taken into account by means of sources of Gaussian white noise that are added to the deterministic network equations, leading to systems of stochastic differential algebraic equations (SDAEs). A crucial property of the arising SDAEs is the large number of small noise sources that are included. As efficient means of their integration we discuss adaptive linear multi-step methods, in particular stochastic analogues of the trapezoidal rule and the two-step backward differentiation formula, together with a new step-size control strategy. Test results including real-life problems illustrate the performance of the presented methods.

1 Transient noise analysis in circuit simulation

The increasing scale of integration, high clock frequencies and low supply voltages cause smaller signal-to-noise ratios. Reduced signal-to-noise ratio means that the difference between the wanted signal and noise is getting smaller. A consequence of this is that the circuit simulation has to take noise into account. In several applications the noise influences the system behaviour in an essentially nonlinear way such that linear noise analysis is no longer satisfactory and transient noise analysis, i.e., the simulation of noisy systems in the time domain, becomes necessary (see [4, 16]). For an implementation of an efficient transient noise analysis in an analog simulator, both an appropriate modelling and integration scheme is necessary (see [3]).

Here we deal with the thermal noise of resistors as well as the shot noise of semiconductors that are modelled by additional sources of additive or multiplicative Gaussian white noise currents that are shunt in parallel to the noise-free elements. Thermal noise i_{th} of resistors is caused by the thermal motion of electrons and is described by Nyquist's theorem. Shot noise i_{shot} of

pn -junctions, caused by the discrete nature of currents due to the elementary charge, is modelled by Schottky's formula and inherits noise intensities that depend on the deterministic currents:

$$i_{th} = \sqrt{\frac{2kT}{R}}\xi(t), \quad i_{shot} = \sqrt{q_e|i_{det}(u)|}\xi(t). \quad (1)$$

Here $\xi(t)$ is a standard Gaussian white noise process, R denotes the resistance, T is the temperature, $k = 1.38 \cdot 10^{-23}$ is Boltzmann's constant, $i_{det}(u)$ is the characteristic of the noise-free current through the pn -junction and $q_e = 1.60 \cdot 10^{-19}$ is the elementary charge.

Combining Kirchhoff's current law with the element characteristics and using the charge-oriented formulation yields a stochastic differential-algebraic equation (SDAE) of the form (see e.g. [15], or for the deterministic case [6])

$$A \frac{d}{dt}q(x(t)) + f(x(t), t) + \sum_{r=1}^m g_r(x(t), t)\xi_r(t) = 0, \quad (2)$$

where A is a constant singular incidence matrix determined by the topology of the dynamic circuit parts, the vector $q(x)$ consists of the charges and the fluxes, and x is the vector of unknowns consisting of the nodal potentials and the branch currents through voltage-defining elements. The term $f(x, t)$ describes the impact of the static elements, $g_r(x, t)$ denotes the vector of noise intensities for the r -th noise source, and ξ is an m -dimensional vector of independent Gaussian white noise sources (see e.g. [4, 16]). One has to deal with a large number of equations as well as of noise sources, where one can and has to exploit the fact that compared to the other quantities the noise intensities $g_r(x, t)$ are small.

Though the system (2) formally differs only by the additional noise term from the deterministic system, a completely different mathematical framework has to be applied. A serious mathematical description begins by introducing the Brownian motion or the Wiener process that is caused by integrating the white noise " $W(t) = \int_0^t \xi(s)ds = \int_0^t dW(s)$ " (see e.g. [1]). Problem (2) is then understood as a stochastic integral equation

$$Aq(X(s))\Big|_{t_0}^t + \int_{t_0}^t f(X(s), s)ds + \sum_{r=1}^m \int_{t_0}^t g_r(X(s), s)dW_r(s) = 0, \quad t \in [t_0, T], \quad (3)$$

where the second integral is an Itô-integral, and W denotes an m -dimensional Wiener process (or Brownian motion) given on the probability space (Ω, \mathcal{F}, P) with a filtration $(\mathcal{F}_t)_{t \geq t_0}$. The solution is a stochastic process depending on the time t and on the random sample ω . The value at fixed time t is a random variable $X(t, \cdot) = X(t)$ whose argument ω is usually dropped. For a fixed sample ω representing a fixed realization of the driving Wiener process, the function $X(\cdot, \omega)$ is called a realization or a path of the solution. Due to the

influence of the Gaussian white noise, typical paths of the solution are nowhere differentiable.

The theory of stochastic differential equations distinguishes between the concepts of strong, i.e., pathwise solutions and weak, i.e., the distribution law of solutions. We decided to aim at the simulation of solution paths, i.e., strong solutions that reveal the phase noise that is of particular interest in case of oscillating solutions. From the solution paths statistical data of the phase as well as moments of the solution can be computed in a post-processing step. We therefore use the concept of strong solutions and strong (mean-square) convergence of approximations.

By the implicitness of the systems (2) or (3) and the singularity of the matrix A the model is not an SDE, but an SDAE. We refer to [15] for analytical results as well as convergence results for certain drift-implicit methods.

In this paper we discuss adaptive linear multi-step methods, in particular stochastic analogues of the trapezoidal rule and the two-step backward differentiation formula, see Section 2. The applied step-size control strategy is described in Section 3. Here we extensively use the smallness of the noise. In Section 4 new ideas for the control both of time and chance-discretization are discussed. Test results including real-life problems that illustrate the performance of the presented methods are given in Section 5.

2 Adaptive numerical methods

The key idea to design methods for SDAEs is to force the iterates to fulfill the constraints of the SDAE at the current time-point. Here we consider stochastic analogues of methods that have proven very useful in the deterministic circuit simulation. Paying attention to the DAE structure, the discretization of the deterministic part (drift) is implicit, whereas the discretization of the stochastic part (diffusion) is explicit.

We consider stochastic analogues of the variable coefficient two-step backward differentiation formula (BDF₂) and the trapezoidal rule, where only the increments of the driving Wiener process are used to discretize the diffusion part. Analogously to the Euler-Maruyama scheme we call such methods multi-step Maruyama methods. The variable step-size BDF₂ Maruyama method for the SDAE (3) has the form (see [11] and, for constant step-sizes, e.g. [2])

$$A \frac{q(X_\ell) + \alpha_{1,\ell} q(X_{\ell-1}) + \alpha_{2,\ell} q(X_{\ell-2})}{h_\ell} + \beta_{0,\ell} f(X_\ell, t_\ell) + \sum_{r=1}^m g_r(X_{\ell-1}, t_{\ell-1}) \frac{\Delta W_r^\ell}{h_\ell} - \alpha_{2,\ell} \sum_{r=1}^m g_r(X_{\ell-2}, t_{\ell-2}) \frac{\Delta W_r^{\ell-1}}{h_\ell} = 0, \quad (4)$$

$\ell = 2, \dots, N$. Here, X_ℓ denotes the approximation to $X(t_\ell)$, $h_\ell = t_\ell - t_{\ell-1}$, and $\Delta W_r^\ell = W_r(t_\ell) - W_r(t_{\ell-1}) \sim N(0, h_\ell)$ on the grid $0 = t_0 < t_1 < \dots < t_N = T$. The coefficients $\alpha_{1,\ell}, \alpha_{2,\ell}, \beta_{0,\ell}$ depend on the step-size ratio $\kappa_\ell =$

$h_\ell/h_{\ell-1}$ and satisfy the conditions for consistency of order one and two in the deterministic case. By construction the scheme has order 1/2 in the stochastic case (see [11]). A correct formulation of the stochastic trapezoidal rule for SDAEs requires more structural information (see [12]). It should implicitly realize the stochastic trapezoidal rule for the so called inherent regular SDE of (3) that governs the dynamical components. Both the BDF₂ Maruyama method and the stochastic trapezoidal rule of Maruyama type have only an asymptotic order of strong convergence of 1/2, i.e.,

$$\|X(t_\ell) - X_\ell\|_{L_2(\Omega)} := \max_{\ell=1,\dots,N} (E|X(t_\ell) - X_\ell|^2)^{1/2} \leq c \cdot h^{1/2}, \quad (5)$$

where $h := \max_{\ell=1,\dots,N} h_\ell$ is the maximal step-size of the grid. For additive noise the order may be 1. This holds true for all numerical schemes that include only information on the increments of the Wiener process.

However, the noise densities given in Section 1 contain small parameters and the error behaviour is much better. In fact, the errors are dominated by the deterministic terms as long as the step-size is large enough [2, 11]. In more detail, the error of the given methods behaves like $\mathcal{O}(h^2 + \varepsilon h + \varepsilon^2 h^{1/2})$, when ε is used to measure the smallness of the noise, i.e., $g_r(x, t) = \varepsilon \hat{g}_r(x, t)$, $r = 1, \dots, m$ where $\varepsilon \ll 1$. Thus we can expect order 2 behaviour if $h \gg \varepsilon$. Higher numerical effort for higher deterministic order pays off only if the noise is *very* small.

3 Local error estimates

The smallness of the noise allows special estimates of the local error terms, which can be used to control the step-size. We aim at an efficient estimate of the mean-square of local errors by means of a number of simultaneously computed solution paths. This leads to an adaptive step-size sequence that is identical for all paths. For the drift-implicit Euler-Maruyama scheme this step-size control has been presented in [10], see also [4, 16].

In [13, 14] the authors extended this strategy to stochastic linear multi-step methods with deterministic order 2 and provided a reliable error estimate. Let \tilde{L}_ℓ approximate the dominating local error in AX_ℓ by

$$\tilde{L}_\ell = c_\ell h_\ell \cdot \left[\frac{2\kappa_\ell}{\kappa_\ell + 1} f(X_\ell, t_\ell) - 2\kappa_\ell f(X_{\ell-1}, t_{\ell-1}) + \frac{2\kappa_\ell^2}{\kappa_\ell + 1} f(X_{\ell-2}, t_{\ell-2}) \right], \quad (6)$$

where c_ℓ is the error constant of the related deterministic scheme. This estimate is based on already computed values of the drift term. Recall that \tilde{L}_ℓ is a vector valued random variable as is the solution X_ℓ . For the measurement of errors we use the mean-square norm in $L_2(\Omega)$. In dependence on the small parameter ε and the step-size h_ℓ the L_2 -norm of the local error behaves like $\mathcal{O}(h_\ell^3 + \varepsilon h_\ell^{3/2} + \varepsilon^2 h_\ell)$. The term of order $\mathcal{O}(h_\ell^3)$ dominates the local error behaviour as long as h_ℓ^3 is much larger than $\varepsilon h_\ell^{3/2}$, i.e., $\varepsilon^{2/3} \ll h_\ell$. Under this condition also the expression $\|\tilde{L}_\ell\|_{L_2}$ approximates the local error.

Depending on the available information we will monitor different quantities to satisfy accuracy requirements,

- i) control $\|(A + h_\ell \beta_{0,\ell} J_\ell)^{-1} \tilde{L}_\ell\|_{L_2}$ to match a given tolerance for X_ℓ ,
- ii) control $\|\tilde{L}_\ell\|_{L_2}$ to match a given tolerance for AX_ℓ , or
- iii) control $\|A^- \tilde{L}_\ell\|_{L_2}$ to match a given tolerance for PX_ℓ .

Here J_ℓ is the Jacobian of the drift function f w.r.t. the first variable, and A^- denotes the pseudo inverse of A , and P is an appropriate projector. Since $(A/h_\ell + \beta_{0,\ell} J_\ell) = 1/h_\ell \cdot (A + h_\ell \beta_{0,\ell} J_\ell)$ is the Jacobian of the discrete scheme (4) this matrix (or a good approximation to it) and its factorization are usually available. In case of M sampled paths, the L_2 -norm in i)–iii) is estimated by using the M values \tilde{L}_ℓ^i , $i = 1, \dots, M$. For example, in case i) we use

$$\left\| (A + h_\ell \beta_{0,\ell} J_\ell)^{-1} \tilde{L}_\ell \right\|_{L_2} \approx \left(\frac{1}{M} \sum_{i=1}^M \left| (A + h_\ell \beta_{0,\ell} J_\ell)^{-1} \tilde{L}_\ell^i \right|^2 \right)^{1/2}. \quad (7)$$

4 A solution path tree algorithm

In the analysis so far, the number M of sample paths has not been specified yet. It influences the sampling error in the approximation of the L_2 -norm in the error estimate (7). We have $\|\tilde{L}_\ell\|_{L_2} = \hat{\eta}_\ell + \vartheta_\ell$, where $\hat{\eta}_\ell$ is the approximation of the dominating local error term based on M sample paths and ϑ_ℓ is the sampling error.

Our aim in tuning the number of paths is to balance the local error and the sampling error. Let d_ℓ be a given upper bound for the sampling error ϑ_ℓ at time t_ℓ , e.g. calculated as an approximation of the higher deterministic error term of order $O(h_\ell^4)$. We then derive the best number M_ℓ of paths by

$$M_\ell = \left\lfloor \frac{1}{d_\ell^2} \frac{\hat{\mu}_\ell^2 \cdot \hat{\sigma}_\ell^2}{\hat{\mu}_\ell^2 + \hat{\sigma}_\ell^2} \right\rfloor, \quad (8)$$

where $\hat{\mu}_\ell$ and $\hat{\sigma}_\ell^2$ are estimates of the mean and the standard deviation of the error estimate at time-point t_ℓ , respectively. Here $\lfloor x \rfloor$ denotes the smallest integer greater or equal to x .

The best number of paths M_ℓ depends on the time-point t_ℓ and is realized by approximate solutions generated on a tree of paths that is extended, reduced or kept fixed adaptively. In [9] the authors describe the construction of a solution path tree in detail. The method uses probabilities π_ℓ^i ($\ell = 1, \dots, N$; $i = 1, \dots, M_\ell$) to weight the solution paths. Figure 1 gives an impression, how a solution path tree looks like. At each time-step the optimal expansion or reduction problem is formulated by means of combinatorial optimization models. The path selection is modelled as a mass transportation problem in terms of the L_2 -Wasserstein metric (see [5] in context of scenario reduction in stochastic programming). The algorithm has been implemented in practice. The results presented in the next section show its performance.

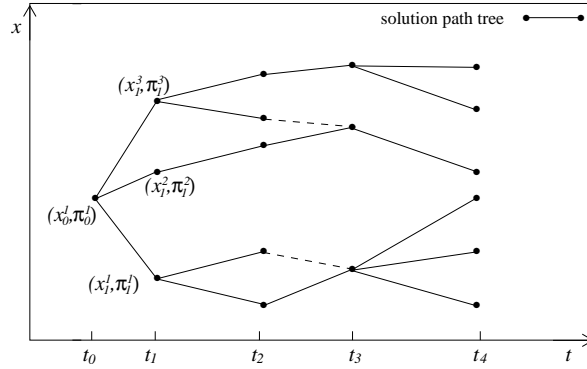


Fig. 1. A solution path tree: Variable time-points t_ℓ , solution states x_ℓ^i and path weights π_ℓ^i .

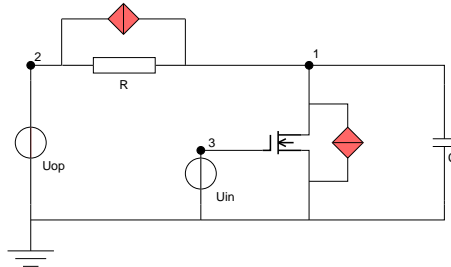


Fig. 2. Thermal noise sources in a MOSFET inverter circuit

5 Numerical results

Here we present numerical experiments for the stochastic BDF₂ applied to two circuit examples. The first one is a small test problem, for which we have used an implementation of the adaptive methods discussed in the previous sections in Fortran code. To be able to handle real-life problems, a slightly modified version of the schemes has been implemented in Qimonda's in-house analog circuit simulator TITAN. The second example shows the performance of this industrial implementation.

A MOSFET inverter circuit

We consider a model of an inverter circuit with a MOSFET transistor, under the influence of thermal noise. The related circuit diagram is given in Figure 2. The MOSFET is modelled as a current source from source to drain that is controlled by the nodal potentials at gate, source and drain. The thermal noise of the resistor and of the MOSFET is modelled by additional white noise current sources that are shunt in parallel to the original, noise-free elements. To highlight the effect of the noise, we scaled the diffusion coefficient by a factor of 1000.

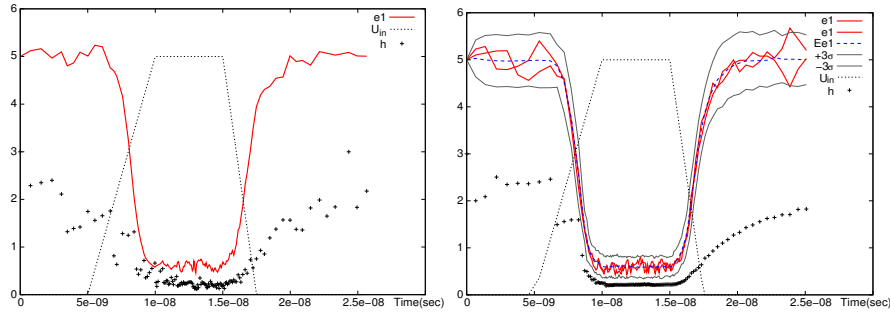


Fig. 3. Simulation results for the noisy inverter circuit:
 1 path 127(+29 rejected) steps; 100 paths 134(+11 rejected) steps

In Figure 3 we present simulation results, where we plotted the input voltage U_{in} and values of the output voltage e_1 versus time. Moreover, the applied step-sizes, suitably scaled, are shown by means of single crosses. We compare the results for the computation of a single path (left picture) with those for the computation of 100 simultaneously computed solution paths (right picture). The additional solid lines show two different solution paths, the dashed line gives the mean of 100 paths and the outer thin lines the 3σ -confidence interval for the output voltage e_1 . We observe that using the information of an ensemble of simultaneously computed solution paths smoothes the step-size sequence and considerably reduces the number of rejected steps, when compared to the simulation of a single path. The computational cost that is mainly determined by the number of computed (accepted + rejected) steps is reduced.

We have applied the solution path tree algorithm to this example. The upper graph in Figure 4 shows the computed solution path tree together with the applied step-sizes. The lower graph shows the simulation error (solid line), its error bound (dashed line) and the used number of paths (marked by \times), vs. time. The maximal number of paths was set to 250. The results indicate that there exists a region from nearly $t = 1 \cdot 10^{-8}$ up to $t = 1.5 \cdot 10^{-8}$ where we have to use much more than 100 paths. This is exactly the area in which the MOSFET is active and the input signal is inverted. Outside this region the algorithm proposes approximately 70 simultaneously computed solution paths.

A voltage controlled oscillator

As an industrial test application we use a voltage controlled oscillator that is a simplified version of a fully integrated 1.3 GHz VCO for GSM in $0.25 \mu\text{m}$ standard CMOS (see [8]). For simulation, the oscillator is embedded in a test environment. The VCO is tunable from about 1.2 GHz up to 1.4 GHz. The unknowns of the VCO in the MNA system are the charges of the six capacities, the fluxes of the four inductors, the 15 nodal potentials and the

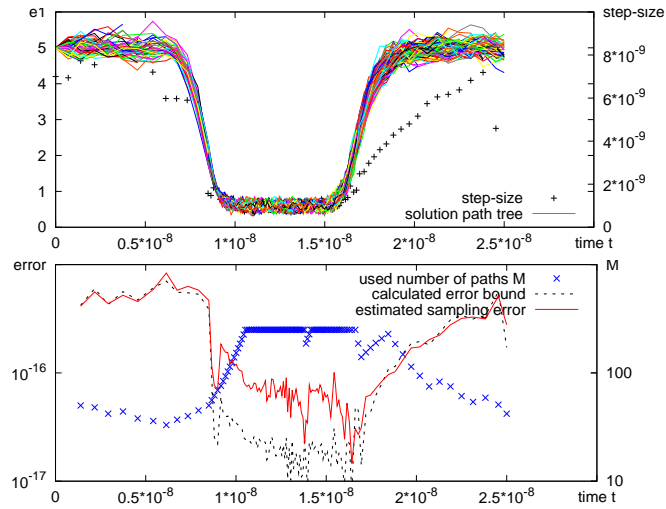


Fig. 4. Simulation results for the noisy inverter circuit: Solution path tree and step-sizes (top), sampling error, its error bound and the number of paths (bottom).

currents through the voltage sources. This circuit contains 5 resistors and 6 MOSFETs, which induce 53 sources of thermal or shot noise. To make the differences between the solutions of the noisy and the noise-free model more visible, the noise intensities had been scaled by a factor of 500.

Numerical results obtained with a combination of the BDF_2 and the trapezoidal rule are shown in Fig. 5, where we plotted the difference of the nodal potential $V(7) - V(8)$ of node 7 and 8 versus time. The solution of the noise-free system is given by a dashed line. Four sample paths (dark solid lines) are shown. They cannot be considered as small perturbations of the deterministic solution, phase noise is highly visible. To analyze the phase noise we performed 10 simultaneous simulations with different initializations of the pseudo-random numbers. In a postprocessing step we computed the length of the first 50 periods for each solution path and then from these the corresponding frequencies. In Fig. 6 the mean μ of the frequencies (horizontal lines), the smallest and the largest frequencies (boundaries of the vertical thin lines) and the boundaries of the confidence interval $\mu \pm \sigma$ (the plump lines) are presented, where σ was computed as the empirical estimate of the standard deviation. The mean appears increased and differs by about $+0.25\%$ from the noiseless, deterministic solution. Further on, the frequencies vacillate from 1.18 GHz (-0.95%) up to 1.21 GHz ($+1.55\%$). So the transient noise analysis shows that the voltage controlled oscillator runs in a noisy environment with increased frequencies and smaller phases, respectively.

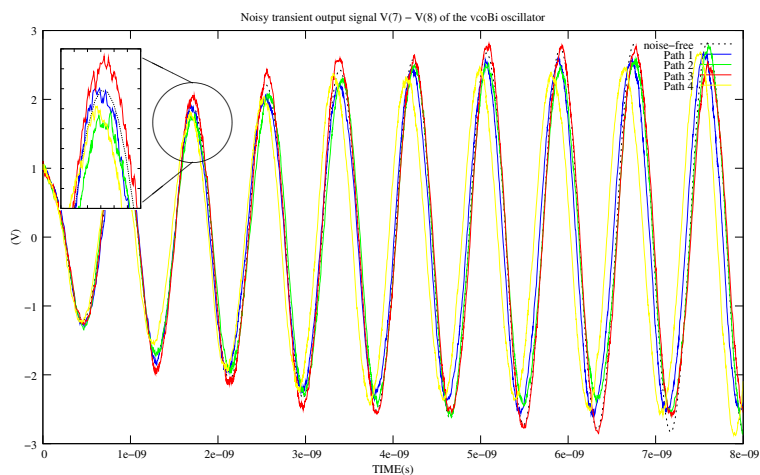


Fig. 5. Noisy transient output signal of a VCO.

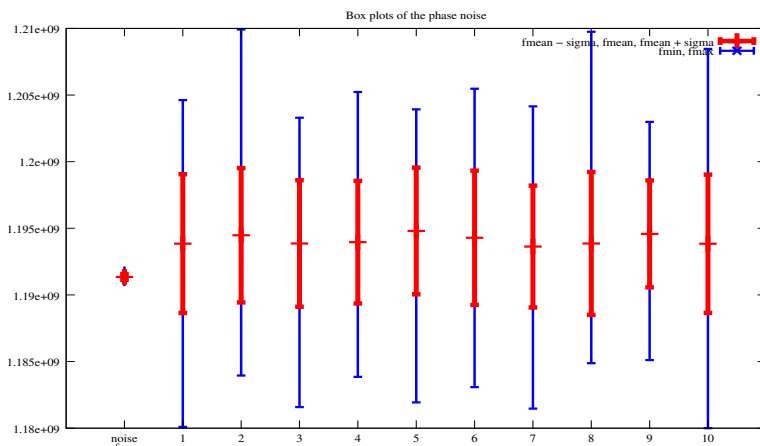


Fig. 6. Boxplots of the phase noise, scaled by a factor of 500

6 Conclusions

Quite similar to deterministic circuit simulation, it is essential to have the application in mind while developing new efficient algorithms. We have presented variable step-size two-step schemes for SDAEs which require only the increments of the driving Wiener process. Though these schemes possess only convergence order $1/2$ from a theoretical point of view, they show order 2 in circuit simulation, as the deterministic terms dominate the errors. This can be considered in the step-size control. Taking the stochastic properties of the circuit into account leads to an increased efficiency of the methods.

An important application of transient noise analysis is to get insight into the statistical properties of the solution paths. We showed that the number of

paths necessary for this purpose varies with the time-points. By implementing a solution path tree algorithm, it is possible to save computing time or to get more accurate outputs compared to a naive approach which would require to calculate all paths over the complete integration interval.

These results allow an efficient transient noise simulation which helps the designer to cope with challenges due to technology progress. Further improvements may include parallelisation and the handling of flicker noise.

References

1. Arnold, L.: Stochastic differential equations: Theory and Applications. Wiley, New York, 1974.
2. Buckwar, E., Winkler, R.: Multi-step methods for SDEs and their application to problems with small noise. *SIAM J. Num. Anal.*, **44**(2), 779–803 (2006)
3. Denk, G.: Circuit simulation for nanoelectronics. In: M. Anile, G. Ali, G. Mascali (Eds.): *Scientific Computing in Electrical Engineering (Mathematics in Industry 9)*, 13–20. Springer, Berlin, 2006.
4. Denk, G., Winkler, R.: Modeling and simulation of transient noise in circuit simulation. *Math. and Comp. Modelling of Dyn. Systems*, **13**(4), 383–394 (2007)
5. Dupačová J., Gröwe-Kuska, N., Römisch, W.: Scenario reduction in stochastic programming. *Math. Program., Ser. A* **95**, 493–511 (2003)
6. Günther, F., Feldmann, U.: CAD-based electric-circuit modeling in industry I. Mathematical structure and index of network equations. *Surv. Math. Ind.*, **8**, 97–129 (1999)
7. Higham, D.J.: An algorithmic introduction to numerical simulation of stochastic differential equations. *SIAM Review*, **43**, 525–546 (2001)
8. Tiebout, M.: A fully integrated 1.3 GHz VCO for GSM in 0.25 μm standard CMOS with a phasenoise of -142 dBc/Hz at 3MHz offset. In: *Proceedings 30th European Microwave Conference, Paris* (2000)
9. Römisch, W., Sickenberger, Th.: On generating a solution path tree for efficient step-size control. In preparation.
10. Römisch, W., Winkler, R.: Stepsize control for mean-square numerical methods for SDEs with small noise. *SIAM J. Sci. Comp.*, **28**(2), 604–625 (2006)
11. Sickenberger, T.: Mean-square convergence of stochastic multi-step methods with variable step-size. *J. Comput. Appl. Math.*, to appear
12. Sickenberger, T., Winkler, R.: Efficient transient noise analysis in circuit simulation. In: *Proceedings of the GAMM Annual Meeting 2006, Berlin, Proc. Appl. Math. Mech.* **6**(1), 55–58 (2006)
13. Sickenberger, T., Weinmüller, E., Winkler, R.: Local error estimates for moderately smooth problems: Part I – ODEs and DAEs. *BIT Numerical Mathematics*, **47**(2), 157–187 (2007).
14. Sickenberger, T., Weinmüller, E., Winkler, R.: Local error estimates for moderately smooth problems: Part II – SDEs and SDAEs. Preprint 07-07, Institut für Mathematik, Humboldt-Universität zu Berlin (2007). Submitted for publication.
15. Winkler, R.: Stochastic differential algebraic equations of index 1 and applications in circuit simulation. *J. Comput. Appl. Math.*, **157**(2), 477–505 (2003)
16. Winkler, R.: Stochastic differential algebraic equations in transient noise analysis. In: M. Anile, G. Ali, G. Mascali (Eds.): *Scientific Computing in Electrical Engineering (Mathematics in Industry 9)*, 151–158. Springer, Berlin, 2006.